17th World Conference on Earthquake Engineering, 17WCEE
Sendai, Japan - September 13th to 18th 2020

REGIONAL-SCALE SEISMIC VULNERABILITY QUANTIFICATION OF PRESTRESSED CURVED BRIDGES

Junwon Seo [1], Jharna Pokhrel [2], Luke Rogers [3]

[1] *Associate Professor (with Tenure) and Chairman of ASCE Timber Bridges Committee, Department of Civil and Environmental Engineering, South Dakota State University, Brookings, SD 57007, USA, e-mail: junwon.seo@sdstate.edu*

[2] *Architectural/Structural Engineer, Gage Brothers, 2810 N. Bahnson Ave., Sioux Falls, SD 57104, USA, e-mail: jpokhrel@gagebrothers.com*

[3] *Bridge E.I.T, HDR, 701 Xenia Ave. South, Suite 600, Minneapolis, MN 55416, USA, e-mail: luke.rogers@hdrinc.com*

Abstract

Given numerous prestressed bridges with a wide range of radius of curvatures in use across all seismic zones, regional-scale seismic vulnerability and the risk of such bridges should be examined. This paper is intended to use surrogate models to efficiently quantify seismic vulnerability characteristics of single-span prestressed curved girder bridge portfolios in the United States. To create a broad spectrum of single-span prestressed curved bridges with variation in structural and geometrical characteristics, an experimental design technique (i.e., Central Composite Design) is employed. Based on the central composite design-based bridge portfolios, details for each bridge are designed according to the American Association of State Highway and Transportation Officials (AASHTO) LRFD Bridge Design Specifications, and analytical models are constructed using finite element analysis software. Then, synthetic ground motions are applied to each model and non-linear time history analyses are completed per model to extract seismic response to the ground motions. Maximum seismic response of key bridge elements, such as bearing and abutment, was captured and used to generate surrogate models using statistical principals. Then, the surrogate models are integrated into Monte Carlo Simulation to treat uncertainty in structural and geometrical parameters and end up the quantification of regional-scale seismic vulnerability for the bridges. Resulting data are analyzed not only to examine seismic susceptibility of the bridges, but also to look into the effects of the various parameters on their seismic vulnerability. Major findings are that the surrogate models are able to rapidly determine the seismic vulnerability of the bridges and that the ratio of span length to radius of curvature (s/r) has an influence on the bridges' vulnerability.

Keywords: prestressed curved bride; seismic vulnerability; surrogate model; span length; radius of curvature

1. Introduction

A bridge has been regarded to be one of the most vulnerable transportation infrastructures during an earthquake in the United States (US) because of its inherent uncertainty in geometry and seismic loads [1]. A bridge with insufficient seismic design details may induce significant damage on individual bridge components, and eventually structural failure of the entire system. In particular, a number of curved bridges with different radii of curvature have been built and in use across all seismic zones in the US [2]. The radii of curvature in a curved bridge can often induce combined torsional and flexure behavior and complex weight distribution, resulting in higher deformation at critical sections of the bridge during seismic excitations [3-5]. Therefore, examining seismic response of such bridges should be prioritized to estimate their seismic vulnerability.

To estimate the seismic vulnerability of bridges (including curved bridges), the probabilities of exceeding a predefined seismic performance threshold for a bridge component or system have been calculated over the past decades [6-9]. Seismic fragility curves in terms of the exceedance probabilities can be created using associated damage functions with the seismic responses from a large number of computational nonlinear time history analyses with a broad range of ground motions [10-11]. The seismic fragility curve-based approach has been deemed as a common methodology for seismic vulnerability assessment of the curved bridges [3-4] and other bridges [10]. Advancements in generating the seismic fragility curves at low computational costs have been achieved by integrating surrogate models such as Response Surface Metamodel (RSM) with Monte Carlo Simulation (MCS) [12-15]. The RSM-MCS approach has been used for the seismic risk and fragility analysis of curved bridges, leading to less seismic simulations while yielding adequate accuracy of results [3-4, 14].

Although there are past studies with the applications of RSM-MCS approach to the seismic fragility curves of curved bridges, this approach is only limited to the curved steel I-girder bridge portfolios. Given a number of prestressed concrete bridges (PSC) with a wide range of radius of curvatures in use across all seismic zones, regional-scale seismic fragility analysis and the risk of such bridges need to be examined. This study aims to use RSMs to efficiently quantify seismic vulnerability characteristics of prestressed curved girder bridge portfolios in the US. This paper is structured into the following sections: Section 2 presents a portfolio of curved PSC bridges that was studied, an overview of the modeling approach used for the fragility curve generation, while Section 3 deals with the RSM approach used in developing RSM functions at critical bridge components. Section 4 provides component- and system-level fragility curves of single-span curved PSC bridges. Finally, Section 5 provides a summary and conclusions on the seismic vulnerability application of RSMs to the PSC bridges.

2. Studied Curved PSC Bridges

To populate a vast diversity of curved PSC bridges with different configurations at low computational cost, the Central Composite Design (CCD) [3], which is a critical experimental design technique, was used through the program JMP [16]. Note, the bridges that were studied were restrained to a single span PSC bridge portfolio so as to increase its fragility analysis efficiency and recognize distinctly the effects of curved bridge parameters within the portfolio. The parameters considered for this study were span length, deck width, and offset. The CCD technique comprises a 2^k factorial design, where each of the parameters contains a lower level, a middle level, and an upper level from the bridge portfolio. **Table 1** lists the considered parameters that were included in the CCD design. Following the single-span PSC bridge design recommendation from the Precast/Prestressed Concrete Institute (PCI) manual [17], a range of the span length from 21.3m to 33.5m was determined, resulting in a variety of possible bridge configurations at a regional level. The deck width consisting of 9.1m, 12.2m, and 18.3m was chosen to take into account various numbers of traffic lanes according to the American Association of State Highway and Transportation Officials (AASHTO) Load and Resistance Factor Design (LRFD) Bridge Design Specifications [18]. Finally, the offset having three levels of 0.15m, 0.30m and 0.45m was used to establish a variety of the

horizontal curvatures based on the recommendation from the PCI manual [17]. As a result of the completion of the CCD-based bridge portfolio, the total number of the PSC bridges with different radii of curvature was 15. To facilitate comparison in seismic fragilities between the 15 bridges, the ratio of span length to radius of curvature (s/r) was taken as an primary RSM input variable, and the ratio was used to break down the bridges into three classes: (1) less than s/r of 0.05 considered as bridge class 1; (2) s/r between 0.05 and 0.10 considered as bridge class 2; and (3) greater than s/r of 0.10 as bridge class 3. Peak Ground Acceleration (PGA) was employed as the controlling RSM parameter for seismic fragility curve generation. **Table 2** shows the single span 15 curved PSC bridges created from the CCD. With the design recommendations from the AASHTO LRFD Specifications [18], each of the bridges was designed at Strength I, Strength III, and Service I limit states. The characteristics for each bridge and its design details can be found elsewhere [19].

Table 1. Three levels of curved PSC bridge characteristics parameters used for CCD.

Parameters	Lower Level	Meddle Level	Upper Level
Span Length (m)	21.3	33.5	48.7
Offset (m)	0.15	0.30	0.45
Deck Width (m)	9.1	12.2	18.3

Table 2. CCD-based 15 curved PSC bridges for RSMs

Bridge No.	Span-to-curvature ratio	Deck width (m)	PGA (g)
1	0.057	9.1	0.1
2	0.057	18.3	0.1
3	0.114	12.2	0.5
4	0.171	9.1	1
5	0.171	18.3	1
6	0.036	12.2	0.1
7	0.073	9.1	0.5
8	0.073	12.2	0.5
9	0.073	18.3	0.5
10	0.109	12.2	1
11	0.025	9.1	0.1
12	0.025	18.3	0.1
13	0.050	12.2	0.5
14	0.075	9.1	1
15	0.075	18.3	1

3. Surrogate Modeling for Seismic Fragility Generation

3.1 3D Finite Element Model

A three-dimensional (3D) finite element (FE) modeling approach developed by Seo and Rogers [20] in CSiBridge v16 [21] was used to determine the seismic response of the CCD-based curved PSC bridges. The approach considered the nonlinearities in the material and structural properties of the PSC bridges using multi-non-linear frame elements with discrete springs. In detail, the approach followed the single beam-column frame elements representing the superstructure, while the substructure was idealized using the nonlinear frame and spring elements. The abutments were modeled using beam-column frame elements with

appropriate cross-sections and material properties, and the bearings were modeled using bilinear plastic springs. A total of 30 synthetic ground motions with PGA values ranging from 0.10 to 1.0g were obtained from the University of New York at Buffalo [22], and the ground motions were applied to the base of the abutment and pier column foundation components in each model. During the analysis, seismic responses at the bearings and abutments were monitored in terms of longitudinal and transverse deformation. More details on the 3D FE modeling approach can be found in the existing publication [20].

3.2 RSM Development

The RSM functions were developed using the three parameters for the curved PSC bridge characteristics with the given PGAs to compute seismic responses at the bearings and abutments in the longitudinal and transverse directions of each bridge. As stated formerly, the 15 curved PSC bridges with varying span length to radius of curvature were used for the 3D FE modelling, and seismic responses of each were extracted through the nonlinear time history analyses of the models. Individual seismic responses, including the maximum longitudinal bearing response, maximum transverse bearing response, maximum longitudinal abutment response, and maximum transverse abutment response, were used as the output parameters in the CCD table for the development of each RSM. Through the least-square analysis of the CCD table with each of the seismic response sets, all RSM models to estimate each response were derived. The RSMs for the mean and the standard deviation of the bearings in the longitudinal and transverse directions are represented in Equations 1, 2, 3, and 4, respectively. To account for uncertainties in seismic response and randomness in bridge structural characteristics associated with ground motions, the final RSM functions are assumed to have standard normal distribution.

$$\hat{y}_{\mu|lng-bearing} = 32.07 - 242.89x_1 + 34.18x_2 - 4.37x_3 - 1168.17x_1x_2 - 1.88x_1x_3 + 0.45x_2x_3 + 4718.13x_1^2 + 86.99x_2^2 + 0.15x_3^2 \quad (1)$$

$$\hat{y}_{\sigma|lng-bearing} = 5.009 - 19.75x_1 + 1.43x_2 - 0.73x_3 - 311.07.56x_1x_2 - 0.61x_1x_3 + 0.09x_2x_3 + 925.59x_1^2 + 32.83x_2^2 + 0.02x_3^2 \quad (2)$$

$$\hat{y}_{\mu|trns-bearing} = -2.37 - 352.6013x_1 + 35.77x_2 + 1.54x_3 - 1072.39x_1x_2 - 5.41x_1x_3 + 0.35x_2x_3 + 5325.98x_1^2 + 68.84x_2^2 - 0.04x_3^2 \quad (3)$$

$$\hat{y}_{\sigma|trns-bearing} = 3.75 - 134.07x_1 + 12.28x_2 - 0.20x_3 - 444.56x_1x_2 - 1.55x_1x_3 + 0.04x_2x_3 + 2119.19x_1^2 + 29.36x_2^2 + 0.009x_3^2 \quad (4)$$

where $\hat{y}_{\mu|lng-bearing}$ is the mean value of maximum longitudinal deformation at the bearings; $\hat{y}_{\sigma|lng-bearing}$ is the standard deviation for the maximum longitudinal deformation at the bearings; x_1, x_2, and x_3 are the s/r ratio, seismic intensity level parameters, and deck width, respectively. Similarly, $\hat{y}_{\mu|trns-bearing}$ and $\hat{y}_{\sigma|trns-bearing}$ are mean and standard deviation value of maximum transverse deformation at the bearings, correspondingly.

As in the bearing-response RSMs development, the identical procedure was followed to develop RSMs for seismic response at the abutments along both the longitudinal and transverse directions. The RSMs for the mean and the standard deviation for determining the maximum abutment seismic deformation in the longitudinal and transverse directions are shown in Equations 5, 6, 7, and 8, respectively.

$$\hat{y}_{\mu|lng-abutmnt} = -0.54 - 39.59x_1 + 8.10x_2 + 0.23x_3 - 73.75x_1x_2 - 0.57x_1x_3 + 0.16x_2x_3 + 418.73x_1^2 + 0.72x_2^2 + 0.008x_3^2 \quad (5)$$

$$\hat{y}_{\sigma|lng-abutmnt} = -0.29 - 6.15x_1 + 2.89x_2 + 0.05x_3 - 4.27x_1x_2 - 0.14x_1x_3 + 0.02x_2x_3 + 44.15x_1^2 - 1.97x_2^2 - 0.001x_3^2 \quad (6)$$

$$\hat{y}_{\mu|trns-abutmnt} = -10.28 + 79.59x_1 + 3.19x_2 + 1.33x_3 + 337.43x_1x_2 + 2.05x_1x_3 + 0.3x_2x_3 + 5325.98x_1^2 + 68.84x_2^2 - 0.04x_3^2 \quad (7)$$

$$\hat{y}_{\sigma|trns-abutmnt} = 3.75 - 134.07x_1 + 12.28x_2 - 0.20x_3 - 444.56x_1x_2 - 1.55x_1x_3 + 0.04x_2x_3 + 2119.19x_1^2 + 29.36x_2^2 + 0.009x_3^2 \quad (8)$$

where $\hat{y}_{\mu|lng-abtmnt}$ is the mean value of maximum longitudinal deformation at the abutments; $\hat{y}_{\sigma|lng-abtmnt}$ is the standard deviation for the maximum longitudinal deformation at the abutments. $\hat{y}_{\mu|trns-bearing}$ and $\hat{y}_{\sigma|trns-bearing}$ are the respective mean and standard deviation value of maximum transverse deformation at the abutments.

3.3 RSM-Aided Fragility Curve Generation

To generate seismic fragility curves utilizing the developed RSMs, it is necessary to integrate the RSMs into Monte Carlo Simulations (MCS) with Probability Density Functions (PDFs) for each of the RSM parameters that needs to be determined. The RSM parameters, including s/r ratio and bridge width, were considered to be random variables associated with their generated PDFs. The s/r ratio and bridge width were taken as random uniform variables within the range of 0 to 0.171 and 9.1m to 18.3m, respectively. Through MATLAB, the MCS was run to generate insights of the seismic response that is quickly estimated from the RSM for each damage limit state. The damage limit states for the considered bridge components encompassed slight, moderate, extensive, and complete damage [23]. Based on past studies for the limit states, Nielson and DesRoches [10] was adopted for this study with their combined limit states using Bayesian theory (see **Table 3**).

The joint RSM-MCS was first used to calculate the exceedance probability of individual bridge components, including the bearings and abutments, for component-level fragility construction. In detail, the MCS was performed with 10,000 trial runs for each PGA value, according to the suggestion on the exceedance probability estimation in the past studies [3-4]. Repetition of the process over different PGAs provided exceedance probability values at all the damage states, and the component-level fragility curves were constructed by fitting a lognormal cumulative density function to the simulation results. Then, the generated component-level fragility curves were combined into a system-level fragility curve that represents the overall seismic vulnerability of the bridges. The detailed information on the system-level fragility curve generation is included in the next section.

Table 3. Damage limit states used for fragility curve generation

Component	Damage States			
	Slight	Moderate	Extensive	Complete
Bearing, longitudinal (mm)	28.9	104.2	136.1	186.6
Bearing, transverse (mm)	28.8	90.9	142.2	195
Abutment transverse/longitudinal (mm)	9.8	37.9	77.2	NA

Note: NA means not available.

4. Seismic Vulnerability Results and Discussion

4.1 Component-Level Fragility

Through the joint RSM-MCS, component-level fragility curves were created for the considered curved PSC bridges to observe the effect of variation in s/r ratio on its regional seismic fragilities. The focus of this

section is on the discussion of the fragility curves for bridge classes 1 and 2 because the exceedance probabilities at all damage states were zero for bridge class 3, except the slight damage state with its exceedance probability of 0.25 at PGA of 1g. The fragility curves for bridge classes 1 and 2 at the bearings in the longitudinal direction for all damage states are shown in **Figures 1a** and **1b**, respectively. **Figures 2a** and **2b** display the fragility curves for bridge classes 1 and 2 in the transverse direction. The median PGA for the bearings in the longitudinal direction at slight damage state is 0.57g and 0.88g for bridge class 1 and bridge class 2, correspondingly. The difference in the fragility curves for bridge classes 1 and 2 at slight damage state is 35%. Similarly, the median PGA for the bearings in the transverse direction for slight damage state is 0.55g and 0.92g for bridge classes 1 and 2, respectively. The difference for the bridge class fragilities is approximately 40% at slight damage state. These curves demonstrate that the effect of s/r ratio on the bearings within the curved PSC bridges in both the longitudinal and transverse directions. Strictly speaking, the larger the s/r ratio is, the lower the fragility is. There is an interesting finding on these curves at moderate damage state, which is that the exceedance probabilities for moderate damage state for bridge class 1 showed a significant increment with PGA values, while it remained unaffected for the other bridge classes.

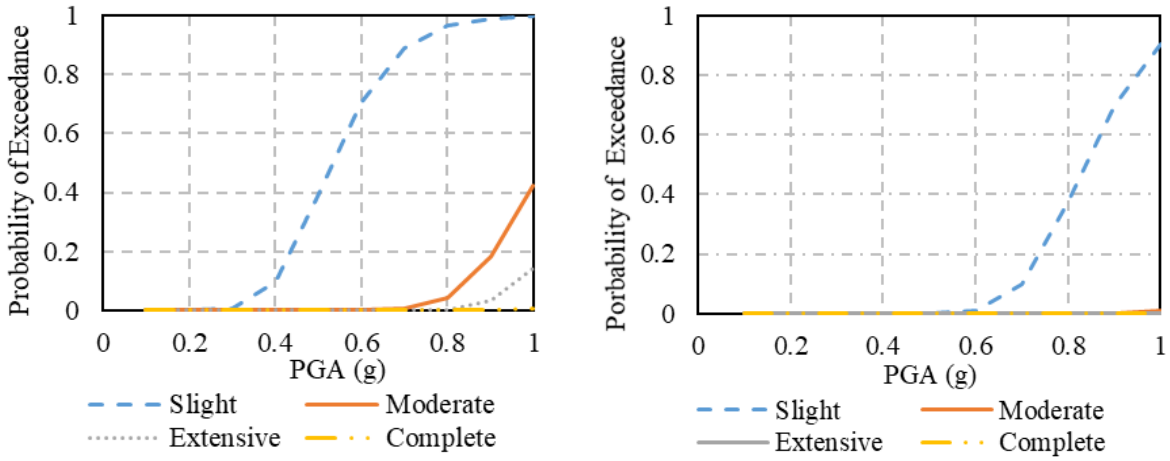

(a) (b)

Figure 1. Component-level seismic fragility curves for curved PSC bridges in the longitudinal direction at bearings: (a) bridge class 1 and (b) bridge class 2.

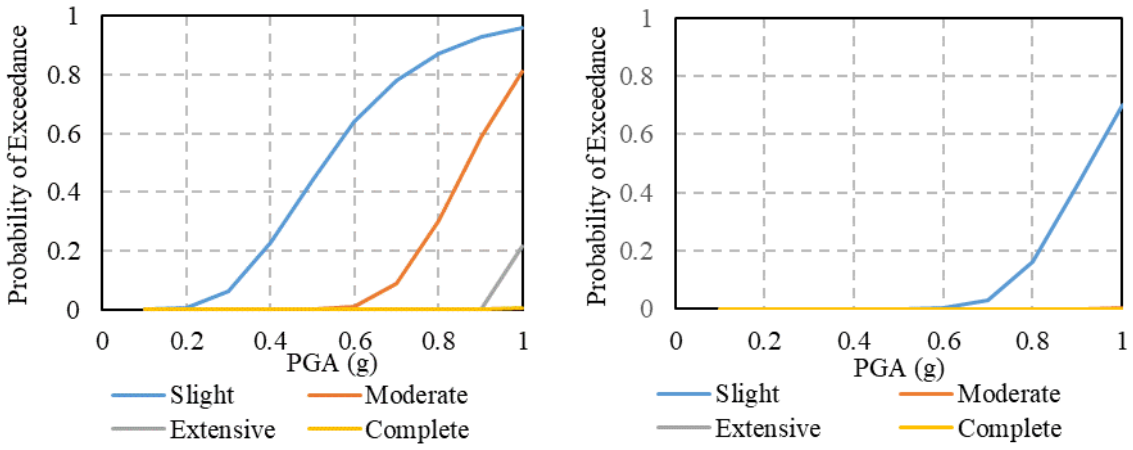

(a) (b)

Figure 2. Component-level seismic fragility curves for curved PSC bridges in the transverse direction at bearings: (a) bridge class 1 and (b) bridge class 2.

To investigate the effect of s/r ratio on the component-level fragility curves of the curved PSC bridges at the abutments, the associated fragility curves were created and analyzed. Note, bridge classes 2 and 3 have zero exceeding probabilities in the component-level fragility curves in both the transverse and longitudinal directions in the range of PGA values; thus, these curves are not included herein. **Figure 3** shows the component-level fragility curves at the abutments for bridge class 1 in the longitudinal and transverse directions, respectively. It appears that the bridge class 1's fragility curves in the longitudinal direction has the exceedance probability of 0.40 at PGA of 1g (slight damage state), while the corresponding value in the transverse direction was 0.77. It turns out that the transverse direction has more significant effects on the abutments' fragilities than the longitudinal direction. As interpreted from the abutments' fragilities for class 1 and the zero fragilities for the other classes, as the s/r ratio decreases, the considered bridges become fragile for the applied ground motion. This trend is somewhat in agreement with the findings derived from the bearing fragility-analysis.

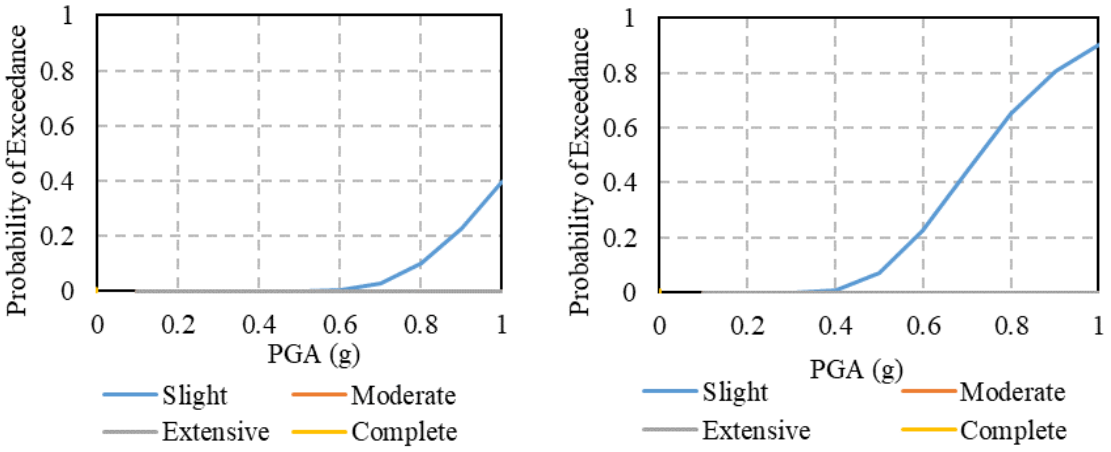

Figure 3. Representative component-level seismic fragility curves at the abutments for bridge class: (a) longitudinal direction and (b) transverse direction.

4.2 System-Level Fragility

To investigate the overall seismic vulnerability of the curved PSC bridges, relevant system-level fragility curves were required for the considered range of s/r ratios. To that end, the exceedance probabilities to each of the bridge components were integrated according to the following equation, resulting in system-level fragility curves for the bridges.

$$max_{i=1}^{m}[P(F_i)] \leq P(F_{sys}) \leq \prod_{i=1}^{m}[1 - P(F_i)] \tag{9}$$

where $P(F_{sys})$ = cumulative probability; and $P(F_i)$ = component level probabilities.

Further information on the generation of system-level fragility curves for curved bridges [20] and other types of bridges [7, 11] using the above equation can be found in past studies. Through the integration of all the component-level fragility curves, the system-level fragility curves for the curved PSC bridges were created for all damage states as illustrated in **Figure 4** for bridge classes 1, 2, and 3. It is obvious that the median exceedance probabilities for bridge class 1 are 0.38g and 0.83g for slight and moderate damage states. For the extensive damage, the maximum exceedance probability is 0.3 at PGA of 1g. In a similar way, for bridge

class 2, the median exceedance probability for slight damage state is 0.65g, while the other damage states have a modicum of effect on the fragilities. The median exceedance probability for bridge class 3 at slight damage state is 0.79g, whereas the remaining damage states have negligible effects on the fragilities. Therefore, it can be concluded that there is an increase in the system-level fragility curves at slight damage state by 41% between bridge classes 1 and 2, and by 17% between bridge classes 2 and 3. Based on all the fragilities at the component and system levels, it is apparent that the curved PSC bridges at the system level is more fragile than its associated components in general.

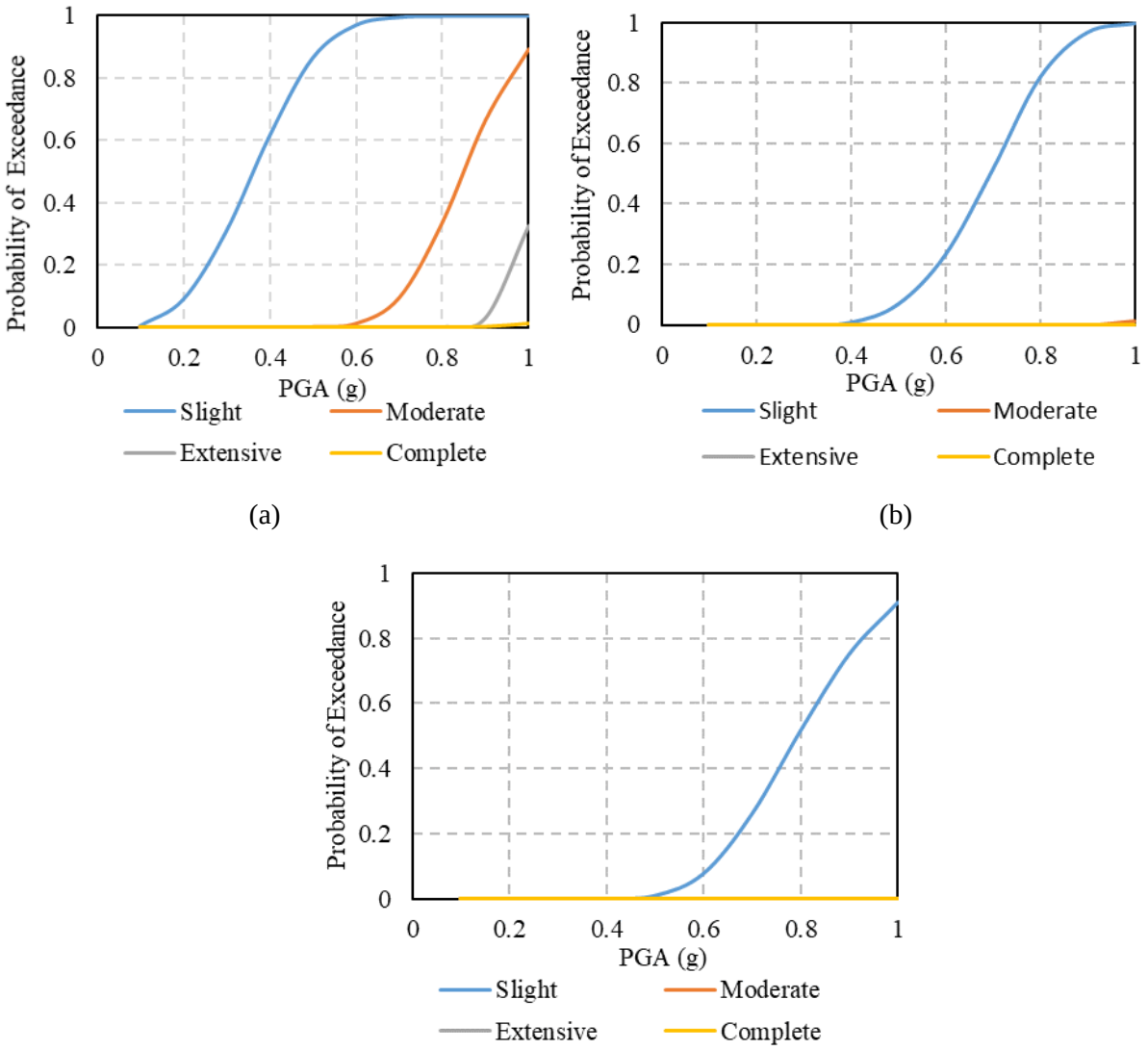

Figure 4: System-level seismic fragility curves for curved PSC bridges: (a) class 1; (b) class 2; and (c) class 3.

5. Conclusions

In this study, Response Surface Metamodels (RSMs) for the single-span curved PSC bridges were developed to efficiently estimate their seismic vulnerability at the component and system levels. To accomplish this, the

experimental Central Composite Design (CCD) design technique was employed to create a wide variety of hypothetical curved PSC bridge configurations with respect to ratio of span length to radius of curvature (s/r) and deck with. Then, the 3D finite element modeling approach was used to model the bridges, and its nonlinear time history analyses were performed using synthetic ground motions in an attempt to capture critical seismic responses on the bearings and abutments of the bridges. Through RSM integrated with Monte Carlo Simulation (MCS) and predefined four damage states, component- and system-level seismic fragility curves were generated. Upon the application of the ground motions to the curved bridges, the seismic vulnerability of the larger s/r ratio decreased. Specifically, the bridges with smaller s/r ratio had lower median PGA values, and the s/r ratio played a significant role in the seismic fragility assessment of the studied curved PSC bridges subjected to the ground motions.

6. Acknowledgments

This work was supported in part by the Funding from the Department of Civil and Environmental Engineering at South Dakota State University.

7. References

[1] Buckle IG (1994): The Northridge, California earthquake of January 11, 1994: performance of highway bridges. *Technical Report NCEER-94-0068*, National Center for Earthquake Engineering Research, USA.

[2] Itani AM, Reno ML (2000): Horizontally Curved Bridges. *Bridge Engineering Handbook*, CRC Press.

[3] Seo J, Linzell D (2012): Horizontally curved steel bridge seismic vulnerability assessment. *Engineering Structures*, 34, 21-32.

[4] Seo J, Linzell D (2013): Use of response surface metamodels to generate system level fragilities for existing curved steel bridges." *Engineering Structures*, 52, 642-653.

[5] Seo J, Linzell D (2013): Nonlinear seismic response and parametric examination of horizontally curved steel bridges using 3D computational models." *ASCE Journal of Bridge Engineering*, 18(3), 220-231.

[6] Shinozuka M, Feng MQ, Kim HK, Kim SH (2000): Nonlinear static procedure for fragility curve development. *ASCE Journal of Engineering Mechanics*, 126(12), 1287-1295.

[7] Nielson BG, DesRoches R (2007): Analytical seismic fragility curves for typical bridges in the central and southeastern United States. *Earthquake Spectra*, 23(3), 615-633.

[8] Padgett JE, DesRoches R (2008): Methodology for the development of analytical fragility curves for retrofitted bridges. *Earthquake Engineering & Structural Dynamics*, 37(8), 1157-1174.

[9] Rogers LP, Seo J (2016): Vulnerability sensitivity of curved precast-concrete I-girder bridges with various configurations subjected to multiple ground motions. *ASCE Journal of Bridge Engineering*, 22(2), 04016118.

[10] Nielson BG, DesRoches R (2007): Seismic fragility methodology for highway bridges using a component level approach. *Earthquake Engineering & Structural Dynamics*, 36(6), 823-839.

[11] Choi E, DesRoches R., Nielson B (2004): Seismic fragility of typical bridges in moderate seismic zones. *Engineering Structures*, 26(2), 187-199.

[12] Ghosh J, Padgett JE, Dueñas-Osorio L (2013): Surrogate modeling and failure surface visualization for efficient seismic vulnerability assessment of highway bridges. *Probabilistic Engineering Mechanics*, 34, 189-199.

[13] Seo J, Dueñas-Osorio L, Craig JI, Goodno BJ (2012): Metamodel-based regional vulnerability estimate of irregular steel moment-frame structures subjected to earthquake events. *Engineering Structures*, 45, 585-597.

[14] Seo J, Park H (2017): Probabilistic seismic restoration cost estimation for transportation infrastructure portfolios with an emphasis on curved steel I-girder bridges. *Structural Safety*, 65, 27-34.

[15] Park J, Towashiraporn P (2014): Rapid seismic damage assessment of railway bridges using the response-surface statistical model. *Structural Safety*, 47, 1-12.

[16] SAS Institute Inc. (2000): *JMP Statistics and Graphics Guide – Version 4.0.3*. Cary, NC.

[17] PCI (2012): *Bridge Design Manual*. Chicago, IL, USA.

[18] AASHTO (2012): *LRFD Bridge Design Specifications*. Washington D.C., USA

[19] Rogers LP (2015): A compilation of research on seismic vulnerability of curved bridges using straight prestressed concrete I-girders. *Master Thesis*, South Dakota State University, Brookings, USA.

[20] Seo J., Rogers, LP (2017): Comparison of curved prestressed concrete bridge population response between area and spine modeling approaches toward efficient seismic vulnerability analysis. *Engineering Structures*, 150, 176-189.

[21] Computers and Structures Inc. (2014): *CSIBridge v16*.

[22] Engineering Seismology Laboratory (2005): *ESL home page*. (http://civil.eng.buffalo.edu/engseislab/index.htm) (Mar. 25, 2014)

[23] FEMA 2003: *HAZUS-MH MR1: Technical Manual, Federal Emergency Management Agency*, Washington, DC.

